

## Self-Consistent Band Structure of Niobium at Normal and Reduced Lattice Spacings

James R. Anderson\*

*University of Maryland, College Park, Maryland 20740*

Dimitrios A. Papaconstantopoulos†

*George Mason University, Fairfax, Virginia 22030*

Joseph W. McCaffrey

*Naval Research Laboratory, Washington, D. C. 20390*

James E. Schirber

*Sandia Laboratories, Albuquerque, New Mexico 07115*

(Received 2 November 1972)

Self-consistent augmented-plane-wave energy-band calculations have been carried out for niobium for (a) normal lattice constant,  $\alpha = 1$  exchange, (b) normal lattice constant,  $\alpha = 2/3$  exchange, and (c) 5% reduced lattice constant,  $\alpha = 2/3$  exchange. At normal lattice constant,  $\alpha = 2/3$  exchange, an occupied  $s$ - $d$ -band width of 0.387 Ry is found, in very good agreement with both  $L$  and  $M$  soft-x-ray emission experiments. The calculated density of states at the Fermi energy is 28.2 states atom<sup>-1</sup> Ry<sup>-1</sup>, corresponding to a McMillan enhancement factor of 1.6. The Fermi surface consists of hole ellipsoids centered at  $N$ , a large hole octahedron centered at  $\Gamma$ , and a multiply connected "jungle gym," similar to that calculated by Mattheiss. The largest difference between experimental and calculated areas is less than 15%.

### I. INTRODUCTION

Although a model for the Fermi surface of niobium was proposed by Mattheiss in 1965,<sup>1</sup> it has been only very recently that single crystals of sufficient perfection have become available to permit detailed Fermi-surface investigations.<sup>2-6</sup> Therefore we have carried out self-consistent band calculations to compare with experiment. Previous calculations by Deegan and Twose<sup>7</sup> and Mattheiss<sup>8</sup> have determined, non-self-consistently, the band structure of Nb using a modified orthogonalized-plane-wave (MOPW) method and the augmented-plane-wave (APW) method, respectively. In both of these calculations the full Slater<sup>9</sup> ( $\alpha = 1$ ) exchange approximation was used.

In the present work we report the results of three self-consistent APW calculations: (a)  $\alpha = 1$  exchange, normal lattice spacing, (b)  $\alpha = \frac{2}{3}$  exchange,<sup>10</sup> normal lattice spacing, and (c)  $\alpha = \frac{2}{3}$ , 5% reduced lattice spacing. The resulting Fermi surface for case (b) is compared to magnetothermal<sup>2</sup> and de Haas-van Alphen<sup>2,3</sup> (dHvA) data. In addition, the logarithmic pressure derivatives of the dHvA frequencies have been calculated from (a) and (b) using an experimental value for the compressibility, and these are compared to very recent pressure results of Anderson and Schirber.<sup>11</sup>

General quantitative agreement is found between our self-consistent  $\alpha = \frac{2}{3}$  results and the non-self-consistent  $\alpha = 1$  energy values of Mattheiss. This interplay of exchange, self-consistency, and configuration has been noted previously<sup>12,13</sup> in the  $3d$  and  $4d$  transition metals.

### II. COMPUTATIONAL PROCEDURES

A description of the APW method may be found in a number of reviews.<sup>13-15</sup> The self-consistency procedure followed in the present work is that of Papaconstantopoulos *et al.*<sup>12</sup> The initial atomic configuration was  $5s^1$ , the same as that used by Mattheiss. The starting ( $\alpha = 1$ ) and self-consistent ( $\alpha = \frac{2}{3}$ ) potentials are shown in Fig. 1. However, we wish to stress a new method for obtaining fast convergence. We have found that averaging the potentials in the usual method,<sup>13</sup>

$$V(r) = 0.75V_{\text{old}}(r) + 0.25V_{\text{new}}(r),$$

gives slow convergence (eight iterations). The situation is improved (five iterations) if the charge densities  $\rho(r)$  are averaged. If, on the other hand, the averaging is done with the quantity  $\sigma(r) = 4\pi r^2 \times \rho(r)$ , only three iterations are needed to converge to within 0.002 Ry. This may be due to the weak  $r$  dependence of  $\sigma(r)$  compared to  $\rho(r)$  and  $V(r)$ . In Fig. 2,  $V(r)$  averaging is compared with  $\sigma(r)$  averaging for two typical states,  $N_2$  and  $H_{12}$ .

The calculations were initially performed on a weighted mesh of 33 points in the full Brillouin zone. For the normal-lattice-constant case, after convergence, two additional iterations were carried out using 128 points in the entire Brillouin zone. These results differed by less than 0.005 Ry from the self-consistent values obtained with the larger mesh. We conclude that the 33-point mesh is usually sufficient for attaining self-consistency.

The Fermi energy was determined by integrating the density of states to five electrons per atom.

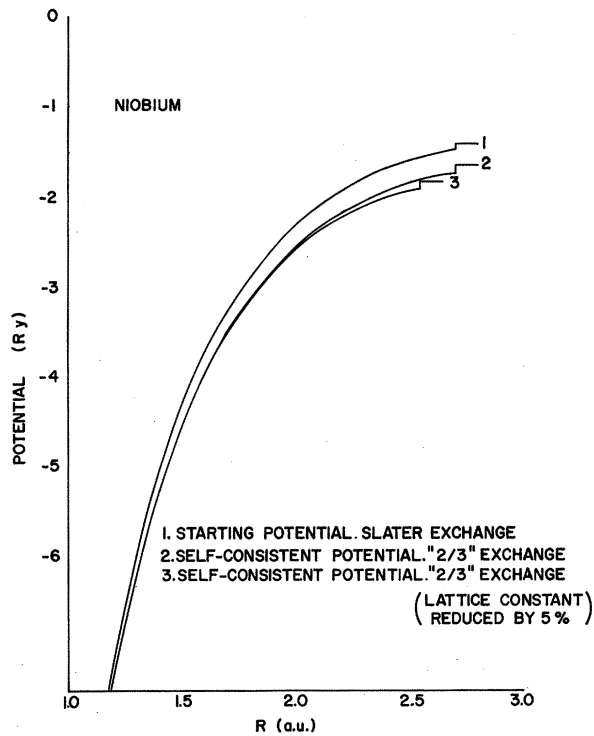


FIG. 1. Starting and final potentials used in self-consistent APW calculations.

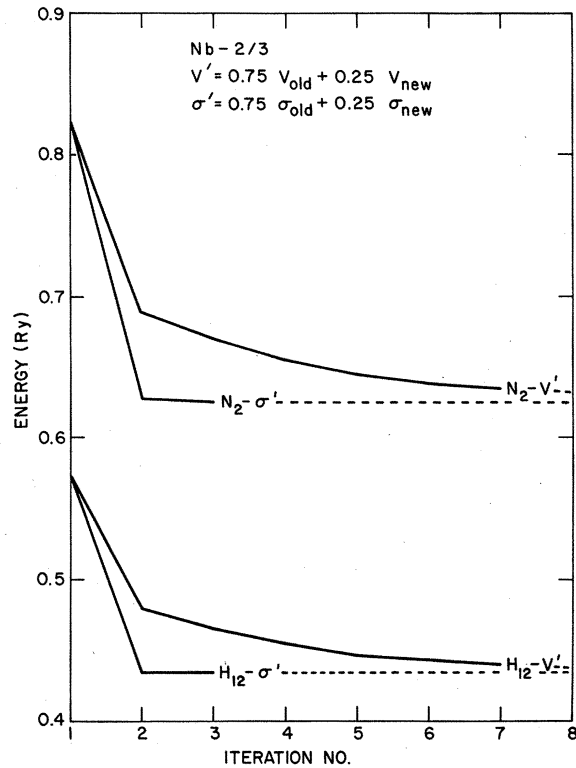


FIG. 2. Convergence rate for  $V(r)$  averaging and  $\sigma(r)$  averaging.

This density of states was found by interpolation of the APW eigenvalues for 48 000 random points in the Brillouin zone.

### III. ENERGY BANDS AND DENSITY OF STATES

In Figs. 3 and 4 we show the self-consistent (SC)  $\alpha = \frac{2}{3}$  energy bands for Nb for normal ( $a_0 = 6.2377$  a.u.<sup>16</sup>) and 5% reduced lattice spacings, respec-

tively. The energy bands are similar to those of the other group-VB transition metals, vanadium<sup>12</sup> and tantalum.<sup>8</sup> As one can see from Figs. 3 and 4 and the summary in Table I, the main differences among the calculations are in the widths and positions of the  $d$  bands. The  $s$ - $d$  separation  $\Gamma'_{25} - \Gamma_1$  and the  $d$ -band width  $H'_{25} - H_{12}$  and  $s$ - $p$ -band width

TABLE I. Energy-band widths (Ry).

		$s$ - $d$ separation		$d$ -band width	Occupied	Occupied	$s$ - $p$ -band width
		$\Gamma'_{25} - \Gamma_1$	$H'_{25} - \Gamma_1$	$H'_{25} - H_{12}$	$d$ -band width	$s$ - $d$ -band width	
					$E_F - H_{12}$	$E_F - \Gamma_1$	$N'_1 - \Gamma_1$
Present calculations							
$\alpha = 1$	SC	0.308	0.634	0.597	0.271	0.308	0.527
$\alpha = \frac{2}{3}$	SC	0.428	0.828	0.755	0.314	0.387	0.553
$\alpha = \frac{2}{3}$ $a = 0.95a_0$	SC	0.424	0.917	0.929	0.397	0.385	0.621
$\alpha = 1$	NSC	0.396	0.752	0.673	0.270	0.349	0.543
Other calculations							
Deegan and Twose <sup>a</sup>		0.440	0.788	0.672	...	...	0.555
Mattheiss <sup>b</sup>		0.420	0.770	0.660	0.28	0.39	0.56
Experiment							
Photoemission <sup>c</sup>					~0.22		
X-ray emission <sup>d,e</sup>						0.37	

<sup>a</sup>Reference 7.

<sup>b</sup>Reference 8.

<sup>c</sup>Reference 19.

<sup>d</sup>Reference 17.

<sup>e</sup>Reference 18.

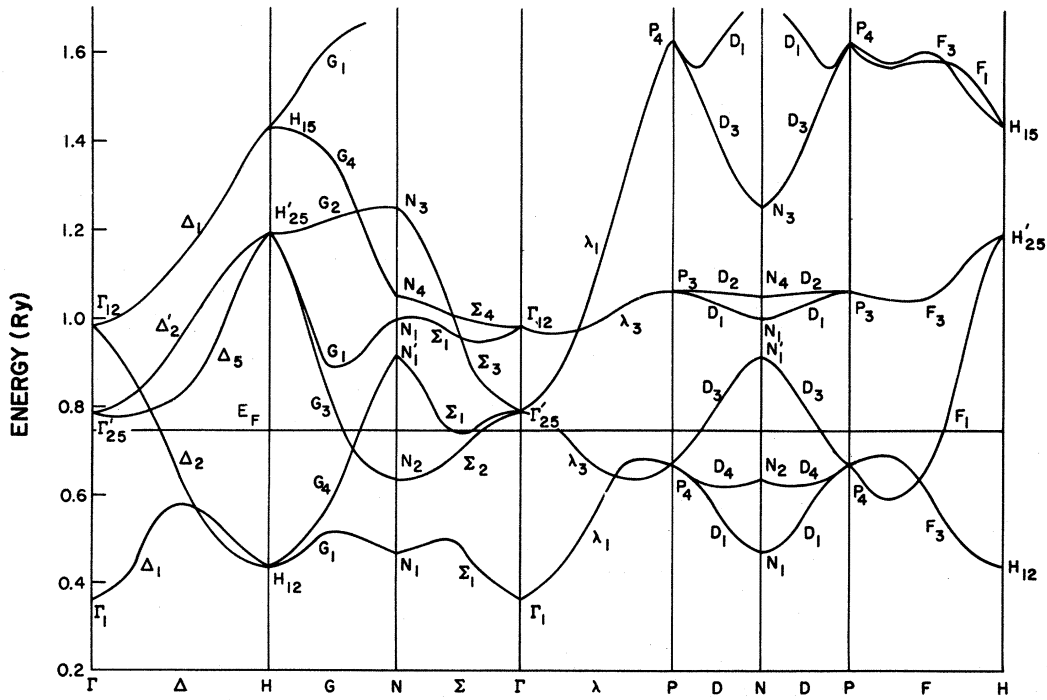


FIG. 3. Energy bands of niobium for  $\alpha = \frac{2}{3}$  at normal lattice constant  $a_0$ .

$N'_1 - \Gamma_1$  are all increased as one goes from Slater to Kohn-Sham exchange. However, a 5% reduction of the lattice constant increases the occupied  $d$ -band width  $E_F - H_{12}$  by  $\sim 30\%$  and the total  $d$ -band

width by  $\sim 20\%$  while leaving the occupied  $s$ - $d$ -band width  $E_F - \Gamma_1$  unchanged.

Although the SC  $\alpha = \frac{2}{3}$   $d$  bands are slightly higher than those given by Mattheiss, the occupied  $s$ - $d$ -

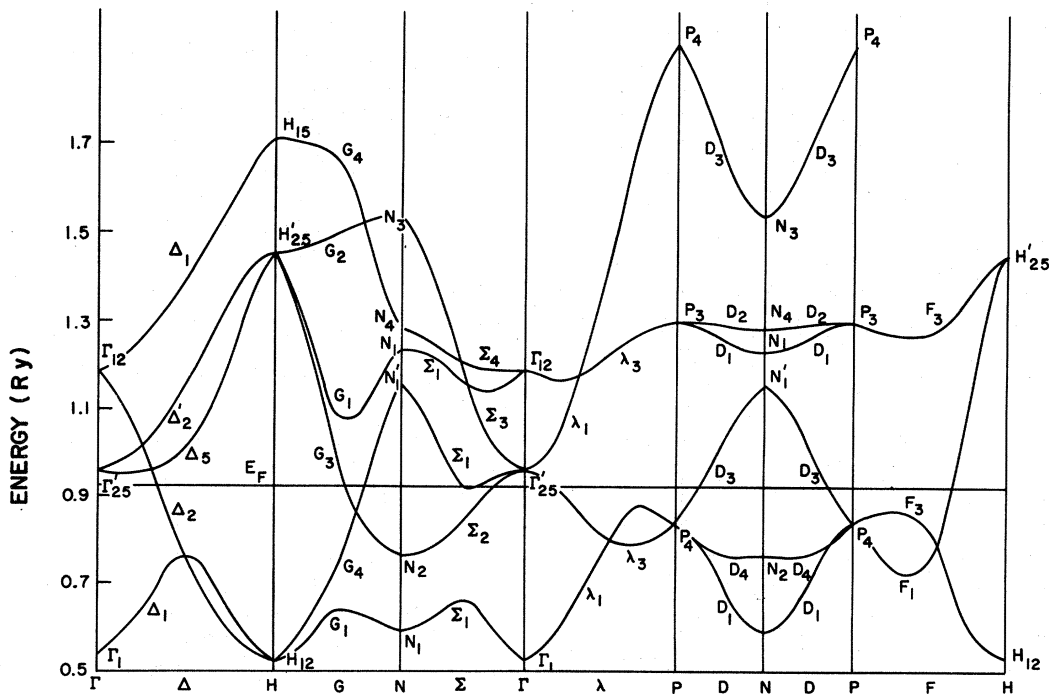


FIG. 4. Energy bands of niobium for  $\alpha = \frac{2}{3}$  at a lattice constant  $a = 0.95a_0$ .

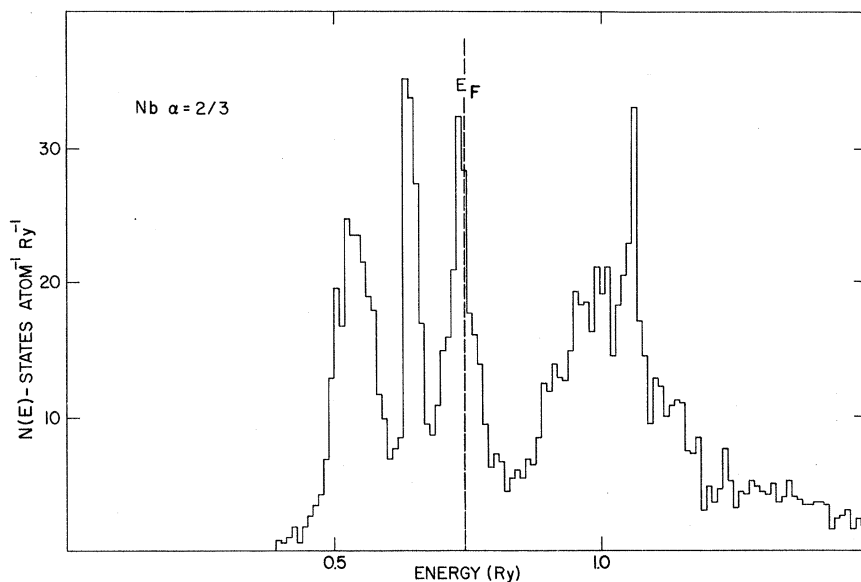


FIG. 5. Density of states of niobium for  $\alpha = \frac{2}{3}$  and normal lattice spacing  $a_0$ .

band widths are about the same. Our non-self-consistent (NSC) results differ from the NSC results of Mattheiss<sup>8</sup> because the two potentials had different discontinuities at the APW sphere radius and Mattheiss used a value for the lattice constant corresponding to 4°K, while we used the room-temperature value.

Except for Fermi-surface data there is very little experimental information by which these calculations can be checked. Both the  $M_V$  soft-x-ray band measured by Holliday<sup>17</sup> and the  $L_{t_2}$  and  $L_{v_1}$  bands measured by Nemoshkalenko and Krivitskii<sup>18</sup> yield an occupied  $s$ - $d$ -band width of about 5 eV (0.37 Ry), in good agreement with the calculated results in Table I. There appears to be structure in the  $M_V$  spectra suggesting that there are peaks in the occupied portion of the density of states. In our calculated density of states, Fig. 5, in addition to a peak near  $E_F$  (about 0.14 eV below), there are peaks at 1.5 and 3.0 eV below  $E_F$ . Eastman<sup>19</sup> has measured photoemission from niobium and reports on occupied  $d$ -band width of about 3 eV, with peaks 0.4, 1.1, and 2.3 eV below  $E_F$ . These peaks correlate fairly well with those in our calculated density of states.

In Fig. 5 it is shown that the density of states at the Fermi energy,  $N(E_F) = 28.2$  states  $\text{atom}^{-1} \text{Ry}^{-1}$ , is nearly a maximum as expected for a high- $T_c$  superconductor. From this result one obtains a value of  $4.79$   $\text{mJ mole}^{-1} \text{K}^{-2}$  for the electronic-specific-heat coefficient. Since the experimental value is  $7.8$   $\text{mJ mole}^{-1} \text{K}^{-2}$ ,<sup>20</sup> an enhancement factor of 1.62 is obtained, in good agreement with McMillan's value of 1.82.<sup>21</sup> In Sec. IV cyclotron-mass-enhancement values are given and the density-of-states enhancement appears to agree well

with the enhancement predicted from magnetothermal oscillations, but the values obtained from de Haas-van Alphen measurements appear to be somewhat large. (See Table II.)

In Fig. 6 the density of states at  $a = 0.95a_0$  is shown, and it can be seen that  $N(E_F)$  has decreased. From this result one might predict a reduced superconducting transition temperature at high pressures, an effect that has been observed by Smith.<sup>22</sup>

#### IV. FERMI SURFACES

The Fermi surfaces at normal and 5% reduced lattice spacings have been calculated from the energy bands by graphical interpolation, and cross sections in the principal symmetry planes are shown in Fig. 7. The results are quite similar to those given by Mattheiss,<sup>8</sup> and we have used his notation to describe the Fermi surface, which consists of hole ellipsoids centered at  $N$  [ELL( $N$ )], a large hole octahedron at  $\Gamma$  [OCT( $\Gamma$ )], and a multiply connected surface of holes called the "jungle gym" (JG). The jungle gym is the source of open orbits observed by Fawcett and co-workers<sup>5,6</sup> and Alekseevskii *et al.*<sup>4</sup>

The cross-sectional areas  $\alpha$  and masses  $m^*/m_0$  have been calculated for some of the extremal orbits, and those results are given in Table II along with some of the experimental information about the Fermi surface. The largest difference between experimental and calculated areas is less than 15% and, since no adjustments have been made in our self-consistent calculation, the agreement seems reasonably good. We may also note from Table II that the non-self-consistent  $\alpha = 1$  calculation of Mattheiss agrees equally well with experiment.

Cyclotron-mass values are also shown in Table II; the results obtained by Mattheiss<sup>8</sup> are included

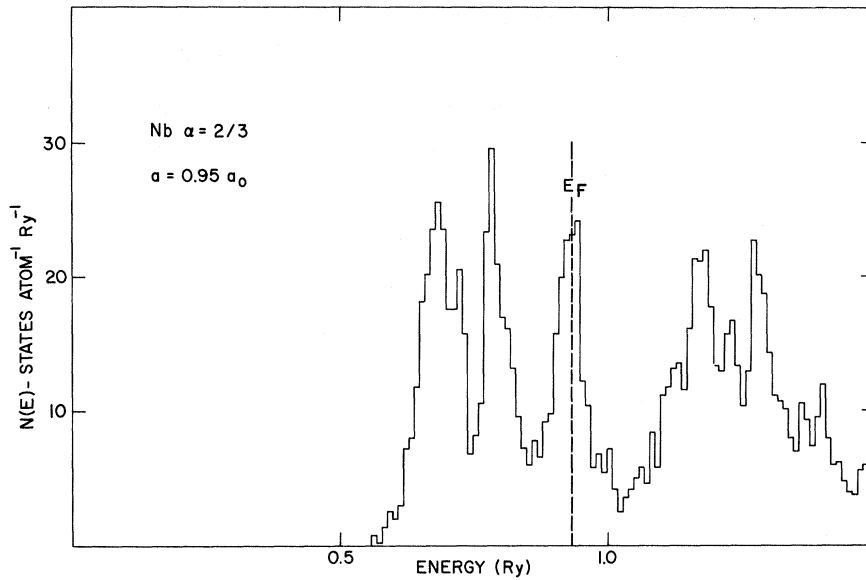


FIG. 6. Density of states of niobium for  $\alpha = \frac{2}{3}$  and at a reduced lattice spacing  $a = 0.95a_0$ .

for comparison. Although there are numerical differences, the trends are the same. However, because we have used graphical construction to determine the masses, our results could be inaccurate by 10–20%.

The mass values have been determined from both de Haas–van Alphen oscillations and magnetothermal oscillations, and there appear to be significant differences between the results from the two experiments which are not understood at present. In Table II we give the enhancement factor—that is, the ratio of the experimental to the calculated mass—for our calculation and both sets of experiments. We note not only that the enhancement factor is rather large but that it appears to be significantly larger for the jungle-gym orbits than for orbits on the ellipsoid. (Table II also shows that the dHvA mass for one of the [111] ellipsoidal sections is unusually large compared to the other ellipsoidal masses. We have no explanation for this at present.)

Finally, we have calculated the logarithmic pressure derivatives of the extremal cross-sectional areas from our APW calculation at  $0.95a_0$ , which corresponds to a pressure of about 260 kbar.<sup>24</sup> In contrast to vanadium,<sup>12</sup> where the ellipsoids at *N* merge with the jungle gym at about 135 kbar, the over-all shape of the Fermi surface does not appear to change in Nb at pressures up to 260 kbar. For three cross sections, measurements have been made of the change in the area with pressure by Anderson and Schirber,<sup>11</sup> and preliminary values are presented in Table II. For the ellipsoids the measured values are about 0.1%/kbar, which is roughly twice the compressibility. The change in the jungle-gym orbit with pressure is very small. In all three cases there is reasonable agreement between calculation and experiment.

#### V. CORE BANDS

The self-consistent potential for  $\alpha = \frac{2}{3}$  was used to calculate the outer core levels *4s* and *4p*. The

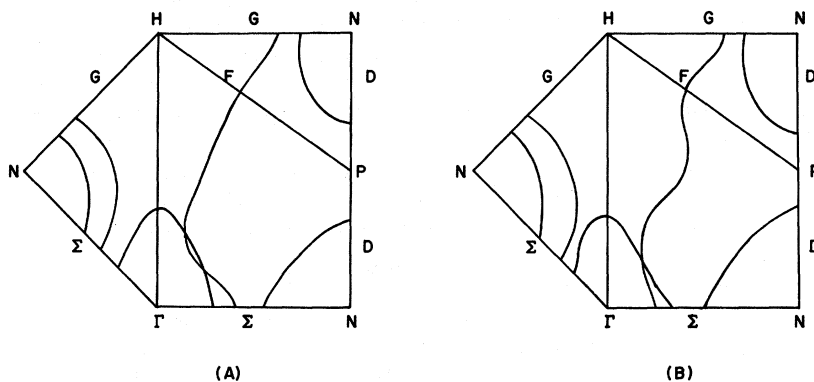


FIG. 7. Fermi surfaces of niobium at  $\alpha = \frac{2}{3}$ . (A) Normal lattice spacing; (B) reduced lattice spacing.

TABLE II. Fermi-surface results.

Surface <sup>a</sup>	Orientation	$\alpha$ ( $\text{\AA}^{-2}$ )		$m^*/m_0$				$\frac{d \ln \alpha}{dP}$ ( $10^{-2}$ kbar <sup>-1</sup> )		
		Experiment		Experiment		Calculation		Experiment <sup>b</sup>		
		I <sup>c</sup>	II <sup>d</sup>	MT <sup>e</sup>	dHvA	I <sup>c</sup>	II <sup>d</sup>	MT	dHvA	
JG	[100]	0.138 <sup>e</sup>			1.6 ± 0.4				3.1 <sup>f</sup>	0.12
		0.139 <sup>f</sup>	0.13	0.117	1.12	0.5	0.57	2.15	2.9 <sup>g</sup>	
OCT( $\Gamma$ )	[100]		0.83	0.881		1.7	1.92			
ELL(N)	[100]	0.639 <sup>e</sup>				0.9	0.83			0.09
ELL(N)	[001]	0.638 <sup>f</sup>								
		0.815 <sup>e</sup>	0.82	0.855	1.60	1.97 ± 0.09 <sup>f</sup>	0.95	0.97	1.69	2.1 <sup>f</sup>
OCT( $\Gamma$ )	[110]	0.813 <sup>f</sup>				1.3	1.66			
		0.760 <sup>e</sup>	0.74	0.675						
ELL( $\Gamma$ )	[110]		0.73	0.762	1.54 ± 0.06 <sup>f</sup>	0.72	0.79		2.1 <sup>f</sup>	0.13
ELL( $\Gamma$ )	[101]	0.757 <sup>f</sup>				1.0	0.98			
		0.857 <sup>e,f</sup>	0.96	0.944						
ELL(N)	[011]	0.657 <sup>e</sup>			1.40 ± 0.06 <sup>f</sup>	0.78	0.70	1.57	1.8 <sup>f</sup>	0.15
JG( $\Gamma$ )	[111]	0.658 <sup>f</sup>	0.71	0.677	1.22	1.52 <sup>g</sup>			1.95 <sup>g</sup>	
		1.862 <sup>e</sup>	0.65	0.742		1.7	2.29			-0.09
JG(H)	[111]	1.860 <sup>f</sup>	1.95	1.881	3.1 ± 0.1 <sup>f</sup>	0.96	1.17	3.2 <sup>f</sup>	< 0.01	0.025
		0.647 <sup>e</sup>	0.38	0.453		1.3	1.54			-0.065
OCT( $\Gamma$ )	[111]		0.62	0.663	1.28	0.72	0.73	1.78	2.2 <sup>f</sup>	0.12
ELL( $\Gamma$ )	[111]	0.644 <sup>f</sup>			1.46 <sup>g</sup>				2.0 <sup>g</sup>	
ELL( $\Gamma$ )	[111]	0.813 <sup>e</sup>	0.79	0.876	2.65 <sup>g</sup>	0.85	1.12	3.1 <sup>g</sup>		0.12
		0.811 <sup>f</sup>								

<sup>a</sup>Notation is an obvious modification of that used by Mattheiss (Ref. 8) (see text).

<sup>b</sup>Reference 11.

<sup>c</sup>Present work.

<sup>d</sup>Reference 8.

<sup>e</sup>Reference 2.

<sup>f</sup>Reference 3.

<sup>g</sup>Reference 23.

resulting bandwidths and those of Deegan and Twose<sup>7</sup> are shown in Table III. It is noted that the present calculation gives greater widths for 4s and 4p bands than the OPW calculation. On the other hand, the gap  $G_1$  between the conduction and the 4s bands and the gap  $G_2$  between the 4s and 4p bands are both smaller than those found by Deegan and Twose. The above workers, in their OPW calculation, treated the 4s and 4p levels as band states rather than localized core states. In our calculation we kept the charge density, corresponding to those levels, constant through the self-consistency cycle. However, it should be interesting to per-

TABLE III. Core widths (Ry).

	4s-band width	4p-band width	$G_1$	$G_2$
Present calculation	0.05	0.12	3.09	1.50
Deegan and Twose <sup>a</sup>	0.03	0.10	3.39	1.65

<sup>a</sup>Reference 7.

form the self-consistent calculation by recomputing at each cycle the 4s and 4p levels.

*Note added in proof.* Recently it was found by Janak *et al.*<sup>25</sup> that for the case of Cu an exchange coefficient  $\alpha = 0.77$  gives the best agreement with experiment. We have also found in the case of vanadium<sup>12</sup> that our results for  $\alpha = \frac{2}{3}$  were consistently lower than the experimental values. We then performed a linear interpolation between the  $\alpha = \frac{2}{3}$  and  $\alpha = 1$  results and predicted that the best agreement will occur at a value of  $\alpha$  higher than the  $X\alpha$  value. However, when we performed the same approximate calculation for Nb, most of the areas of the Fermi surface tend to worsen the good agreement with experiment which the  $\alpha = \frac{2}{3}$  value gives.

## ACKNOWLEDGMENTS

We wish to acknowledge the support of the University of Maryland Computer Science Center and, in particular, the assistance of George Baltz of

this Center. We also wish to thank Miss F. L. Cheng for help with the computations. We also

thank Dr. Crabtree, Dr. Ketterson, and Dr. Windmiller for sending us their data prior to publication.

- \*Supported in part by the Advanced Research Projects Agency.  
<sup>†</sup>Supported in part by the National Science Foundation.  
<sup>1</sup>L. F. Mattheiss, Phys. Rev. **139**, A1893 (1965).  
<sup>2</sup>M. M. Halloran, J. M. Condon, J. E. Graebner, J. E. Kunzler, and F. S. L. Hsu, Phys. Rev. **B 1**, 369 (1970).  
<sup>3</sup>G. B. Scott and M. Springford, Proc. R. Soc. A **320**, 115 (1970).  
<sup>4</sup>N. E. Alekseevskii, K. Kh. Bertel, and A. V. Dubrovin, Zh. Eksp. Teor. Fiz. Pis'ma Red. **10**, 116 (1969) [JETP Lett. **10**, 74 (1969)].  
<sup>5</sup>W. A. Reed and R. R. Soden, Phys. Rev. **173**, 677 (1968).  
<sup>6</sup>E. Fawcett, W. A. Reed, and R. R. Soden, Phys. Rev. **159**, 533 (1967).  
<sup>7</sup>R. A. Deegan and W. D. Twose, Phys. Rev. **164**, 997 (1967).  
<sup>8</sup>L. F. Mattheiss, Phys. Rev. **B 1**, 373 (1970).  
<sup>9</sup>J. C. Slater, Phys. Rev. **81**, 385 (1951).  
<sup>10</sup>R. Gaspar, Acta Math. Acad. Sci. Hung. **3**, 263 (1954); W. Kohn and L. J. Sham, Phys. Rev. **140**, A1133 (1965).  
<sup>11</sup>J. R. Anderson and J. E. Schirber (unpublished).  
<sup>12</sup>D. A. Papaconstantopoulos, J. R. Anderson, and J. W. McCaffrey, Phys. Rev. **B 5**, 1214 (1971).  
<sup>13</sup>J. O. Dimmock, Solid State Phys. **26**, 103 (1971).  
<sup>14</sup>T. L. Loucks, *Augmented-Plane-Wave Method* (Benjamin, New York, 1967).  
<sup>15</sup>L. F. Mattheiss, J. H. Wood, and A. C. Switendick, Methods Comput. Phys. **8**, 63 (1968).  
<sup>16</sup>W. B. Pearson, *Lattice Spacings and Structure of Metals and Alloys* (Pergamon, New York, 1958).  
<sup>17</sup>J. E. Holliday, in *The Electron Microprobe*, edited by T. D. McKinley, K. F. J. Meinrich, and D. B. Wittry (Wiley, New York, 1966), p. 10.  
<sup>18</sup>V. V. Nemoshkalenko and V. P. Krivitskii, Ukr. Fiz. Zh. **13**, 1274 (1968) [Ukr. Phys. J. **13**, 911 (1969)].  
<sup>19</sup>D. E. Eastman, Solid State Commun. **7**, 1697 (1969).  
<sup>20</sup>F. Heininger, E. Bucher, and J. Muller, Phys. Kondens. Mater. **5**, 243 (1966).  
<sup>21</sup>W. L. McMillan, Phys. Rev. **167**, 331 (1968).  
<sup>22</sup>T. F. Smith, Phys. Lett. A **33**, 465 (1970).  
<sup>23</sup>G. Crabtree, J. B. Ketterson, and L. R. Windmiller (private communication).  
<sup>24</sup>The compressibility  $K_T$  of Nb at 4.2 °K has been obtained from the elastic constants of K. J. Carroll [J. Appl. Phys. **36**, 3689 (1965)]. The value is  $5.78 \times 10^{-4}$  kbar<sup>-1</sup>.  
<sup>25</sup>J. F. Janak, A. R. Williams, and V. L. Moruzzi, Phys. Rev. **B 6**, 4367 (1972).

## Probing the Electron-Phonon Interaction in Potassium by Far-Infrared Cyclotron Resonance

S. J. Allen, Jr., L. W. Rupp, Jr., and P. H. Schmidt

*Bell Laboratories, Murray Hill, New Jersey 07974*

(Received 29 November 1972)

To probe the electron-phonon interaction in potassium, Azbel'-Kaner cyclotron resonance has been observed at four frequencies in the far infrared (29.69, 32.12, 45.407, and 58.25 cm<sup>-1</sup>). The experiments were performed on a novel reflection cavity spectrometer with balanced homodyne detection driven by a c.w. far-infrared laser. Signals are seen for E<sub>1</sub>H and E<sub>2</sub>H at 29.69 and 32.12 cm<sup>-1</sup>, but only for E<sub>1</sub>H at 45.407 and 58.25 cm<sup>-1</sup>. Two effects distinguish cyclotron resonance in potassium in the infrared from that observed at microwaves. First, since the resonant electron does not escape the skin depth before the infrared field changes phase, the resonances suffer from retardation effects and are no longer amenable to the usual Azbel'-Kaner or Chambers theory of cyclotron resonance. Second, there is a strong enhancement of the electron-phonon relaxation rate due to the large density of phonon states available to scatter the excitations when the laser frequency is near the Debye frequency,  $\approx 75$  cm<sup>-1</sup>. The line-shape analysis, used to extract the electron-phonon coupling parameter  $\lambda$ , does not reproduce all of the observed features. In particular, it does not reproduce absorption features on the high-field side of the subharmonic resonance which are shown to be related to the cyclotron waves that propagate across the magnetic field in the bulk. Nevertheless, by focusing attention on the breadth and position of the leading edge of the resonance, we can extract an electron-phonon  $\lambda$ .  $\lambda$  is found to be  $0.11 \pm 0.02$  and agrees with that determined by the temperature dependence of the phonon-limited dc resistivity.

### I. INTRODUCTION

Electrons in normal metals form a strongly interacting gas whose transport properties are best formulated in terms of quasiparticles.<sup>1</sup> Quasiparticles, as conceived by Landau,<sup>1,2</sup> represent

the low-lying collective excitations of the interacting electron system, and behave very much like the electrons from which they were constructed—with one important exception. Whereas the electron lifetime is extremely short, the quasiparticle motion is long lived. Since the quasiparticle state is